arXiv:1610.06444v1 [nucl-th] 20 Oct 2016

Theoretical approaches to low energy $\bar{K}N$ interactions

Aleš Cieplý[1,⋆] and Maxim Mai[2]

[1] *Nuclear Physics Institute, 250 68 Řež, Czechia*
[2] *The George Washington University, 725 21st St. NW, Washington, DC 20052, USA*

Abstract. We provide a direct comparison of modern theoretical approaches based on the SU(3) chiral dynamics and describing the low energy $\bar{K}N$ data. The model predictions for the $\bar{K}N$ amplitudes and pole content of the models are discussed.

1 Introduction

In our contribution we review the current status of low energy $\bar{K}N$ interactions and concentrate on comparison of the available theoretical approaches derived from the effective SU(3) chiral Lagrangian that describes the interaction of the pseudoscalar meson octet with the ground state baryon octet. In the $S = -1$ sector the involved meson-baryon coupled channels are $\pi\Lambda$, $\pi\Sigma$, $\bar{K}N$, $\eta\Lambda$, $\eta\Sigma$ and $K\Xi$ with threshold energies from about 1250 to 1810 MeV. Since the $\Lambda(1405)$ resonance lies closely below the $\bar{K}N$ threshold the chiral perturbation series does not converge in its vicinity and coupled-channel re-summation techniques are standardly employed to sum the major part of the chiral expansion to obtain the scattering amplitude.

In our recent work [1] we performed a direct comparison of the theoretical approaches that include NLO corrections to the leading order in the chiral expansion and fix the free model parameters, the low energy constants, to reproduce the experimental data on K^-p scattering and reactions including the recent precise measurement of kaonic hydrogen characteristics (the shift and width of the $1s$ level due to strong interaction) by the SIDDHARTA collaboration [2]. The discussed models comprise of

- the Kyoto-Munich [3] and Murcia [4] approaches, which rely on the re-summation of the S-wave projected chiral potential. Both are conceptually identical but differ in their treatment of the experimental data and fitting procedures. In our analysis, we have included the NLO models $\mathrm{KM_{NLO}}$ from Ref. [3] and the models $\mathrm{M_I}$ and $\mathrm{M_{II}}$ from Ref. [4].
- the Bonn approach [5] that does not rely on partial wave projection of the interaction kernel when solving the Bethe-Salpeter equation. In Ref. [5], two solutions (which we denote as $\mathrm{B_2}$ and $\mathrm{B_4}$ here) of the global fits to the K^-p experimental data were found compatible with the photoproduction data measured by the CLAS collaboration [6].
- the Prague approach [7] that differs from the other considered approaches by relying on effective separable meson-baryon potentials with off-shell form factors that also regularize the intermediate state Green function, which is equivalent to dimensional regularization used in the other approaches. In our analysis we use the NLO model $\mathrm{P_{NLO}}$, originally denoted as NLO30 in Ref. [7].

⋆ e-mail: cieply@ujf.cas.cz

We refer the reader to the original papers [3], [4], [5] and [7] for the specific details of the considered approaches. Without dwelling upon any technicalities we proceed with a presentation of our findings in the next section and conclude the paper with a brief summary.

2 Results and discussion

The considered models represent the current state of theory on low energy meson-baryon interactions in the $S = -1$ sector and describe the $K^- p$ reactions data about equally well. This is demonstrated in the left panel of Fig. 1 which shows the theoretical predictions for the $1s$ level characteristics of the kaonic hydrogen, the energy shift $\Delta E(1s)$ and the absorption width $\Gamma(1s)$, both caused by the strong interaction. The rectangular areas drawn in the figure visualize the experimental progress with the rectangular boxes covering areas within one standard deviation of the experimental data taken from the KEK [8], DEAR [9] and SIDDHARTA [2] measurements. The theoretical approaches reproduce the most recent SIDDHARTA data quite well and are in very close agreement among each other. However, the same cannot be said concerning the positions of the poles assigned to the $\Lambda(1405)$ resonance and shown in the right panel of Fig. 1. All models based on the chiral SU(3) dynamics generate invariably two poles in the $\pi\Sigma$-$\bar{K}N$ coupled channels sector. The models agree on the real part of the complex energy for the pole that couples more strongly to the $\bar{K}N$ channel and is generated at a higher energy of about 1420 MeV. Though, the imaginary part of the pole energy is not established so well and the position of the second pole varies from one model to another, apparently not constrained much by the experimental data. It was already shown in Ref. [5] that the new CLAS data on $\pi\Sigma$ photoproduction off proton [6] provide additional constrains on the pole positions. On the other hand, the theoretical models still find it difficult to explain the peaks in the $\pi\Sigma$ mass spectra observed in the pp collisions by the HADES experiment [10].

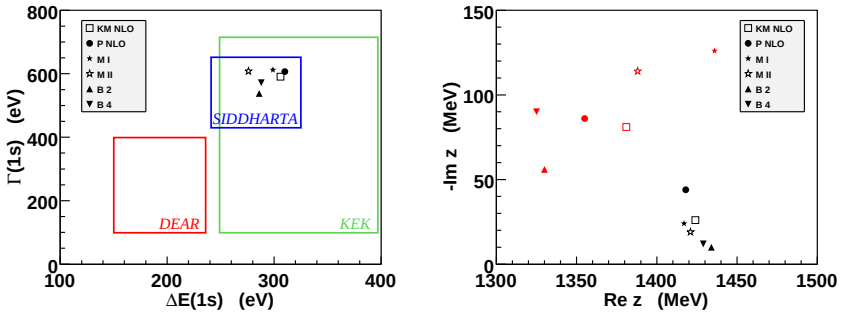

Figure 1. Kaonic hydrogen characteristics (left panel) and positions of the poles assigned to $\Lambda(1405)$ (right panel) as generated by various theoretical approaches.

In Fig. 2 we also demonstrate that the considered approaches lead to very different predictions for the $K^- p$ amplitude extrapolated to sub-threshold energies as well as for the $K^- n$ amplitude. The theoretical ambiguities observed below the $\bar{K}N$ threshold are much larger then those standardly indicated by uncertainty bounds derived from variations of the $K^- p$ scattering length within constraints enforced by the kaonic hydrogen data, see e.g. Ref. [3].

Finally, in Ref. [1] we have also analyzed the origin of the poles of the scattering T-matrix generated by the theoretical models. There, we followed the pole movements to the so-called zero coupling

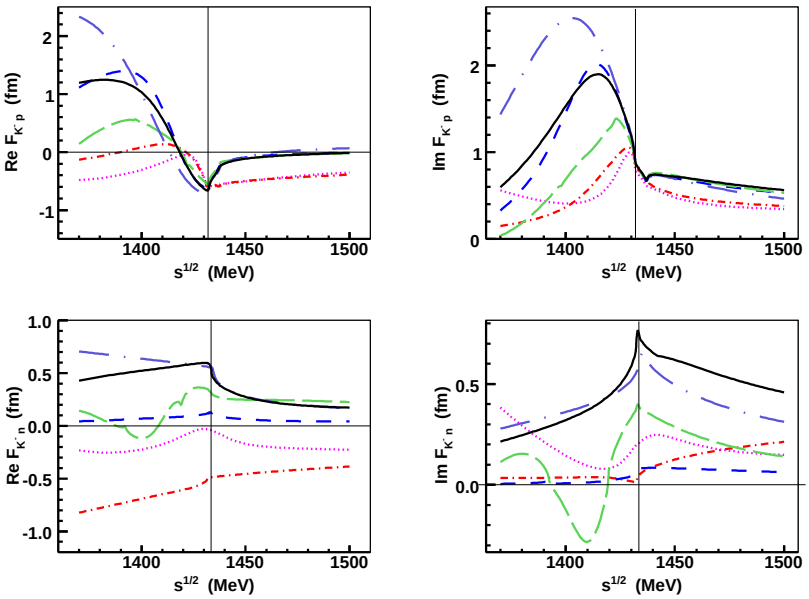

Figure 2. The $K^- p$ (top panels) and $K^- n$ (bottom panels) elastic scattering amplitudes generated by the NLO approaches considered in our work. The various lines refer to the models: B_2 (dotted, purple), B_4 (dot-dashed, red), M_I (dashed, blue), M_{II} (long-dashed, green), P_{NLO} (dot-long-dashed, violet), KM_{NLO} (continuous, black).

limit (ZCL), in which the inter-channel couplings are switched off. Our findings are reviewed in the Table 1 that shows the channels in which a pole assigned to a given resonance persists when the ZCL is reached. As there are two poles assigned to the $\Lambda(1405)$ we present them separately with the indexes 1 and 2. In the complex energy plane the $\Lambda_1(1405)$ pole is usually found at lower energy and further from the real axis than the $\Lambda_2(1405)$ pole. All models have the $\Lambda_1(1405)$ pole in the $\pi\Sigma$ channel when the inter-channel interactions are switched off. The $\Lambda_2(1405)$ pole couples most strongly to the $\bar{K}N$ channel, so it came as a surprise that the pole origin can be traced to the $\eta\Lambda$ channel in the ZCL for the B_2 and M_{II} models. Thus, the other models that have the ZCL pole in the $\bar{K}N$ channel should be preferred if one anticipates a simplified picture of a $\bar{K}N$ bound state submerged in the $\pi\Sigma$ continuum [11]. We have also hinted in Ref. [1] at quite large NLO couplings occurring in the Bonn and Murcia models and being most likely responsible for an appearance of the $\eta\Lambda$ bound state in the ZCL.

In the isoscalar sector the models can also account for the $\Lambda(1670)$ resonance that emerges from the $K\Xi$ pole found in the ZCL. We have argued in Ref. [1] that an appearance of such pole is related to a particular condition imposed on a subtraction constant (or an inverse range in case of the Prague approach). If the condition is not met, the pole is missing as happens for the KM_{NLO} and B_2 models. One should note, however, that with an exception of the Murcia approach the other approaches did not aim at describing the experimental data in the $\Lambda(1670)$ energy region, so it is not surprising that the pole is either completely missing or not at an appropriate position in those models.

Similarly, in the isovector sector the models can provide a pole which can be related to the $\Sigma(1750)$ resonance and the origin of this pole can be traced to the $K\Xi$ virtual (or bound) state in the ZCL. Several of the discussed models also predict an isovector $\bar{K}N$ pole located below the $\bar{K}N$ threshold at the Riemann sheet which is physical in the $\pi\Sigma$ and unphysical in the $\bar{K}N$ channel (it would be the third

Table 1. The origins (channels) of the poles generated by the considered models in which the poles are found when inter-channel couplings are switched off.

		Models					
		P_{NLO}	KM_{NLO}	M_I	M_{II}	B_2	B_4
Resonances	$\Lambda_1(1405)$	$\pi\Sigma$	$\pi\Sigma$	$\pi\Sigma$	$\pi\Sigma$	$\pi\Sigma$	$\pi\Sigma$
	$\Lambda_2(1405)$	$\bar{K}N$	$\bar{K}N$	$\bar{K}N$	$\eta\Lambda$	$\eta\Lambda$	$\bar{K}N$
	$\Lambda(1670)$	$K\Xi$	—	$K\Xi$	$K\Xi$	—	$K\Xi$
	$\bar{K}N(I=1)$	$\bar{K}N$	$\eta\Sigma$	$\bar{K}N$	$\bar{K}N$	—	—
	$\Sigma(1750)$	$K\Xi$	—	$K\Xi$	$K\Xi$	—	$K\Xi$

Riemann sheet if only these two channels were coupled). This pole emerges from an isovector $\bar{K}N$ virtual state generated in the ZCL by the Prague and Murcia models, though the Kyoto-Munich model has it in the $\eta\Sigma$ channel. We note that an existence of this pole was already witnessed in Refs. [12], [13] and [14]. It is understood that it relates to the cusp structure in the energy dependence of the elastic K^-n amplitude obtained for both, the P_{NLO} and the KM_{NLO} models as seen in Fig. 2.

3 Summary

In the present work different versions of the modern chiral unitary approaches were compared directly for the first time. Our main observations are as follows:

- We have demonstrated that the available theoretical models lead to very different predictions for the elastic K^-p and K^-n amplitudes at sub-threshold energies.
- The tracking of the poles to the ZCL provides us with new insights related to the appearance of poles in a given approach. The procedure also reveals different concepts of forming the $\Lambda(1405)$.
- Several models predict an existence of an isovector pole close to the $\bar{K}N$ threshold.

The authors acknowledge a collaboration with U.-G. Meißner and J. Smejkal who contributed to Ref. [1] the current presentation is based on.

References

[1] A. Cieplý, M. Mai, U.-G. Meißner and J. Smejkal, Nucl. Phys. A **954**, 17 (2016)
[2] M. Bazzi *et al.* [SIDDHARTA Collaboration], Phys. Lett. B **704**, 113 (2011)
[3] Y. Ikeda, T. Hyodo and W. Weise, Nucl. Phys. A **881**, 98 (2012)
[4] Z. H. Guo and J. A. Oller, Phys. Rev. C **87**, 035202 (2013)
[5] M. Mai and U.-G. Meißner, Eur. Phys. J. A **51**, 30 (2015)
[6] K. Moriya *et al.* [CLAS Collaboration], Phys. Rev. C **87**, 035206 (2013)
[7] A. Cieplý and J. Smejkal, Nucl. Phys. A **881**, 115 (2012)
[8] M. Iwasaki *et al.*, Phys. Rev. Lett. **78**, 3067 (1997)
[9] G. Beer *et al.* [DEAR Collaboration], Phys. Rev. Lett. **94**, 212302 (2005)
[10] G. Agakishiev *et al.* [HADES Collaboration], Phys. Rev. C **87**, 025201 (2013)
[11] T. Hyodo and W. Weise, Phys. Rev. C **77**, 035204 (2008)
[12] J. A. Oller and U.-G. Meißner, Phys. Lett. B **500**, 263 (2001)
[13] D. Jido, J. A. Oller, E. Oset, A. Ramos and U.-G. Meißner, Nucl. Phys. A **725**, 181–200 (2003)
[14] A. Cieplý, E. Friedman, A. Gal, D. Gazda and J. Mareš, Phys. Rev. C **84**, 045206 (2011)